ACS Photonics

Article

pubs.acs.org/journal/apchd5

Ultrafast Carrier Dynamics of a Photo-Excited Germanium Nanowire−Air Metamaterial

Yanying Li,[†] Raphael Clady,[‡] Ann F. Marshall,[§] Junghyun Park,[∥] Shruti V. Thombare,[∥] Gerentt Chan,[⊥] Timothy W. Schmidt,[#] Mark L. Brongersma,[∥] and Paul C. McIntyre*[,∥]

[†]Department of Applied Physics, [§]Geballe Laboratory for Advanced Materials, [∥]Department of Materials Science and Engineering, and [⊥]Department of Chemistry, Stanford University, Stanford, California United States

[‡]School of Chemistry, University of Sydney, Sydney, NSW, Australia

[#]School of Chemistry, UNSW, Sydney, NSW, Australia

ABSTRACT: Ultrafast carrier dynamics in arrays of single crystal and relatively uniform-diameter Ge nanowires (NWs) are investigated by transient absorption measurements and effective medium simulations. We present the first quantitative analysis of a Ge NW−air metamaterial, translating the photon response of the assemblies to carrier dynamics. Three time regimes of the ultrafast recombination process are identified: Auger recombination dominant (0−5 ps), "fast" surface trapping and recombination dominant (5−20 ps), and a mix of "fast" recombination and "slow" surface trapping (20−200 ps). The rates of surface recombination and their dependences on pump fluence are determined, highlighting the different interactions of electrons and holes with Ge NW surface and interface states. Structural and excitation conditions can be engineered to extend the photogenerated electron and hole lifetimes. Small wire diameters and low pump powers enhance the electron lifetime because charging of defect states in the surface oxide layer produces a potential barrier for electrons to be trapped at Ge/GeO_x interface. This phenomenon simultaneously causes an enhancement of hole lifetime for relatively large wire diameters and large pump powers.

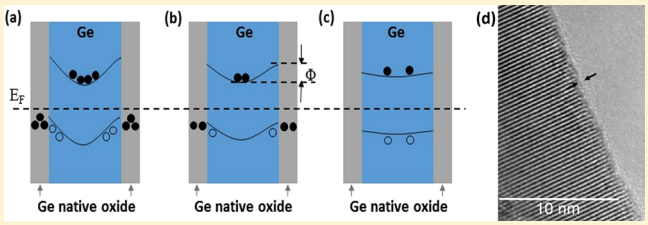

KEYWORDS: *germanium, nanowires, ultrafast, metamaterial, carrier dynamics*

Nanostructured semiconductors have been investigated in recent years due, in large part, to their unique electronic and optical properties emerging from their anisotropic geometry, large surface-to-volume ratio, and their ability to confine electronic carriers. The observed size- and geometry-dependent properties of these nanostructures make them suitable for a broad range of applications. Among these, nanoscale germanium (Ge) wires, particularly, can be used as building blocks for advanced optoelectronic applications, such as lasers,[1−3] light emitters,[4,5] photoresistors,[6] and photodetectors.[7−10] Although such sophisticated devices have been demonstrated, the investigation of the fundamental ultrafast carrier dynamics of semiconductor nanowire (NW) assemblies is so far limited to a small group of materials[11−13] and to qualitative analysis.[14,15] A quantitative translation of the photon response of NW assemblies to carrier dynamics in these structures is essential to exploit them in the design of nanoscale optoelectronic devices.

In this work, we study carrier dynamics in arrays of single crystal and relatively uniform-diameter Ge NWs by ultrafast transient absorption experiments and effective medium simulations. The carrier dynamics of Ge NW assemblies within 200 ps after excitation are very sensitive to the presence of surface states; therefore, the dynamics show a strong dependence on both the NW diameter and the excitation power. The effects of NW diameter on carrier dynamics are investigated and indicate a surface-mediated recombination process dominating during periods 5−200 ps after the pump pulse. This finding is generally consistent with several prior reports on surface recombination in semiconductor NWs.[13,14,16] Here we present the first quantitative analysis of a Ge NW−air metamaterial using the photon response of the assemblies to determine carrier dynamics. This analysis enables us to identify three time regimes for ultrafast recombination processes: Auger recombination (0−5 ps after photoexcitation), recombination via carrier trapping at fast surface states on the nanowires (5−20 ps), and recombination via both fast and slow surface traps (20−200 ps). The rates of surface recombination and their dependence on pump fluence are estimated, and an analysis of the impact of slow states, associated with defects in the surrounding GeO_x native oxide coating of the wires, is presented. These results highlight the distinct interactions of electrons and holes with NW surface states, thus providing insights into (1) the effects of surface defect passivation on semiconductor NWs and (2) the design principles for nanoscale optoelectronic devices.

Germanium NWs were grown to ∼7 μm length via the vapor−liquid−solid (VLS) mechanism using presized colloidal

Received: March 24, 2015
Published: July 1, 2015

DOI: 10.1021/acsphotonics.5b00147
ACS Photonics 2015, 2, 1091−1098

Au nanoparticle catalysts. The diameters of Ge NWs are determined by, and slightly larger than, the diameters of the Au catalysts due to Au particle coarsening prior to wire nucleation. Figure 1a shows a representative SEM image of the vertically

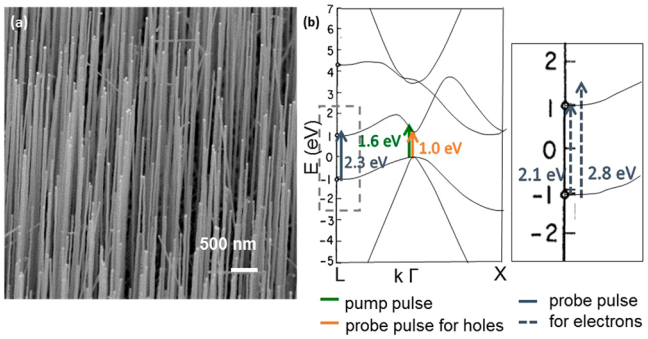

Figure 1. (a) SEM image of vertically aligned Ge NWs grown on Si (111) substrates using 40 nm Au colloids. (b) Schematic Germanium band diagram with pump and probe energy labeled. The zoom-in diagram shows probe pulses, with energy 2.1− 2.8 eV (450−600 nm), for electrons in L-valley of conduction band.

aligned, dense Ge NWs under investigation. The spacing between NWs is small compared to the wavelength of light in the air and substrate and this enables an effective medium analysis of the optical measurements provided in this paper.

Femtosecond pump−probe spectroscopy is an ultrafast optical method allowing separate measurement of electron and hole dynamics in indirect semiconductor nanostructures by selecting the appropriate probe wavelength according to the electronic band structure. In this work, we probe carrier dynamics in Ge NWs whose diameters are greater than or equal to 20 nm. In the case of Ge NWs, it has been shown that the bulk band structure allows a quantitatively accurate interpretation of data obtained from NW diameters larger than 10 nm.[17,18] The schematic bulk Ge electronic band structure in Figure 1b shows the conduction band minimum at L and the corresponding indirect band gap of 0.66 eV. Because excited electrons are scattered to the L-valley within a few ps after above-band gap excitation, hole and electron dynamics can be studied by ultrafast transient absorption (TA), tuning the probe wavelength in the near IR range (1−1.5 μm, 0.8−1.2 eV) for holes and, in the visible range (450−600 nm, 2.1−2.8 eV), for electrons.[14,19] In a bulk indirect gap semiconductor, such as Ge, carrier lifetime is typically in the range of microseconds to milliseconds, much longer than that of a direct gap semiconductor like GaAs. However, nonradiative recombination at surface states, which plays an important role in semiconductor NWs, can reduce carrier lifetime greatly. For Ge NWs, the effects of two populations of defect states associated with the nanowire surface are discussed in detail in this report.

In previous research, it has been shown that state-filling induced transient bleaching and free-carrier transient absorption govern the spectra of reflected probe illumination in the visible range (450−600 nm, 2.1−2.8 eV).[20] Transient absorption dominates in the shorter wavelength regime, reflecting a process in which electrons excited by the pump pulse are excited again by the probe from states near the conduction band edge to higher available states.[20]

RESULT AND DISCUSSION

Optical-pump (780 nm, 1.6 eV), visible/near-IR probe experiments were performed on Ge NW assemblies with different, well-controlled (Ge NWs prepared and grown under the same conditions used in this study and with 40 nm diameter Au colloid catalysts have a diameter distribution of 59.15 ± 5.36 nm (1σ)) diameters to study carrier relaxation in these systems. Comparing experiments on Ge NWs with solid Au catalyst at their tips, to Ge NWs after selective removal of Au using a tri-iodide wet etch chemistry, we found the difference in carrier relaxation to be negligible. It has been reported that surface states have a dominant effect on electrical properties compared to Au impurity atoms in VLS-grown Ge NWs.[21] Figure 2 depicts measurements of hole (1200 nm

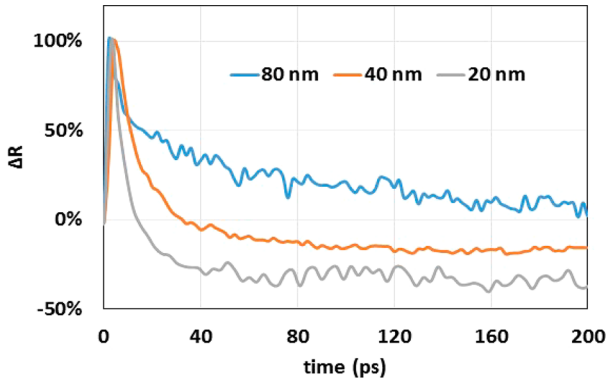

Figure 2. Optical pump−probe measurements on Ge NWs with different diameters (20, 40, and 80 nm). The pump wavelength was 780 nm (1.59 eV), and the probe wavelength was set to 1200 nm (1.03 eV) to probe hole dynamics. The pump fluence was around 500 μJ·cm^{-2}. The differential reflection traces are normalized to the maximum in each trace to compare the temporal behavior.

probe, see Figure 1b) dynamics in samples prepared with 80, 40, and 20 nm diameter Au nanoparticles at a pump fluence of 500 μJ·cm^{-2}. After pumping, excited holes occupy states near the valence band edge. When probe pulses with 1200 nm wavelength (1.0 eV) are incident, the absorption is limited and the reflected signal is therefore increased compared with that before pumping, because the states are occupied. This is known as the state-filling induced bleaching. As excited holes populate these states and recombine from them, the reflected signal increases, providing a probe of hole dynamics.

In Figure 2, the detected differential reflection traces, normalized to the maximum in each trace to compare the temporal behavior, are plotted. The fast signal rise for each sample is due to the initial photoexcitation of holes into energy states in the valence band which are probed by time-delayed 1200 nm (1.0 eV) pulses, while the subsequent signal decay results from relaxation of holes out of these states. As clearly shown in Figure 2, the hole lifetime decreases with the NW diameter, confirming a surface-mediated recombination mechanism.[13,14] Previous studies have indicated that there are two distinct types of surface states on air-exposed Ge crystals. Fast states, physically located at the interface between Ge and its native oxide, have a carrier capture time shorter than a microsecond, and they are chiefly responsible for nonradiative carrier recombination.[14,21−23] For bulk Ge crystals with native oxide, fast surface states include an electron trap 0.24 eV below the conduction band edge and two hole traps 0.17 and 0.22 eV

DOI: 10.1021/acsphotonics.5b00147
ACS Photonics 2015, 2, 1091−1098

above the valence band edge.[24] Slow states, existing in the Ge native oxide layer, have carrier trapping times that vary from a microsecond to hundreds of seconds.[13,22,23,25] The large surface-to-volume ratio of semiconducting nanowires makes them extremely sensitive to surface states that can trap carriers, and several studies indicate that fast surface states[14,21−23] are primarily responsible for nonradiative carrier recombination. The negative signal observed in Figure 2 for longer time delays does not recover within the 1 ns measurement time window used in our experiments. A similar negative reflectivity signal has been observed previously[14] and is likely due to the induced absorption of probe photons by trapped carriers that do not have an opposite charge with which to recombine.

There have been several studies concerning the diameter-dependent surface recombination rate in semiconductor NWs.[13,14,26] However, few reports contain analysis of the excitation-dependence of the surface recombination rate. Here, we present a detailed analysis of the impact of excitation power on electron and hole concentration decay. Figure 3a and b demonstrate, respectively, hole (1200 nm probe, 1.0 eV) and electron (550 nm probe, 2.3 eV) dynamics for different pump

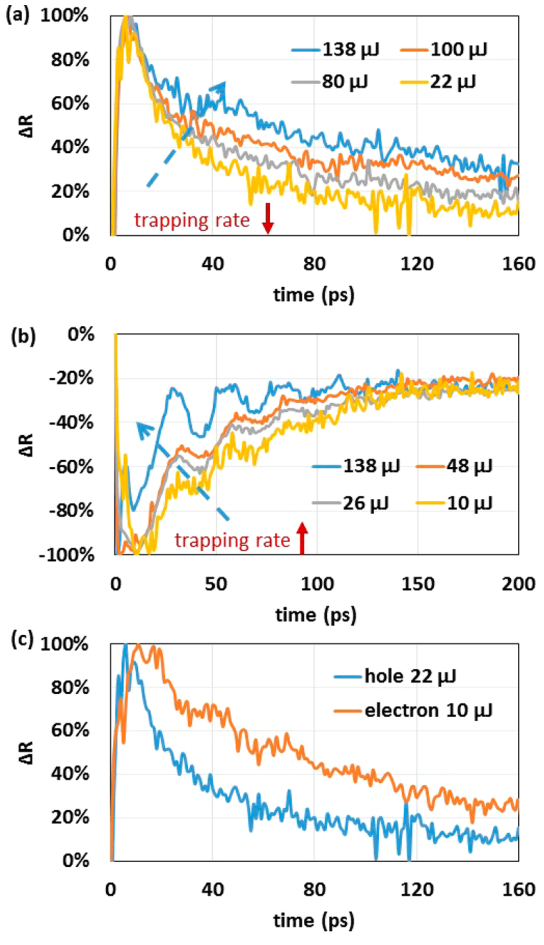

Figure 3. Comparison of (a) hole (1200 nm probe, 1.03 eV) and (b) electron (550 nm probe, 2.25 eV) dynamics in 80 nm NWs for different pump power with a fixed beam spot size of 4 mm^2. For increasing pump intensity (marked by dashed arrow), hole lifetime increases while electron lifetime decreases. (c) Normalized hole and electron dynamics under low pump power. The differential reflection traces are normalized to the maximum in each trace to compare the temporal behavior.

powers in 80 nm diameter Ge nanowire samples with a fixed beam spot size of 4 mm^2. Figure 3a shows that, after photoexcitation, state-filling induces a bleach for the 1200 nm wavelength (1.0 eV) probe. Holes are excited into the valence band after the pump pulse; however, the same excitation of holes is prohibited for the 1200 nm (1.0 eV) probe pulse because the final states have already been occupied by excited holes. This leads to a decrease of absorption, showing a transient bleaching in the spectra. Similar bleaching of interband optical transitions has been observed in both single semiconductor NWs[11,27] and in ensembles.[12,14,28] On the other hand, Figure 3b shows free electron induced absorption immediately after the pump pulse. This phenomenon occurring during absorption of the probe pulse is the further excitation of already excited electrons, from states near the conduction band edge to available higher energy states. These results indicate that the state filling effect observed in Figure 3a is caused by free holes in the valence band, while the free carrier induced absorption in Figure 3b is produced by free electrons in the Ge conduction band (L-valley). The oscillations in Figure 3b result from the transient excitation of acoustic phonons in the NWs after exposure to the intense pump pulse.[20] As expected, the oscillation magnitudes increase as excitation power increases.

Full spectra of the probe-wavelength dependent reflectivity versus time (not shown) for electrons (520−720 nm probe; 1.73−2.39 eV) confirm the increasing decay rate with pump fluence observed in Figure 3b. Hole and electron dynamics were examined in different sample sets of Ge NW assemblies, with controlled NW diameters deposited over a period of several months. They were tested with a range of pump fluence from 10 s of $\mu J/cm^2$ to several mJ/cm^2 and exhibited the same trends shown in Figures 2 and 3, indicating the reproducibility of the sample preparation and pump−probe characterization methodologies.

Despite the fact that transient absorption behavior for electrons and holes is associated with different physical phenomena, recovery of the reflectivity signal monitors the dynamics of carrier trapping at fast surface states. It is interesting to note that, as shown in Figure 3a,b, the rates at which holes and electrons are trapped are, respectively, decreasing and increasing functions of carrier density. This can be explained by the influence of the slow surface states and the resulting band bending near the NW surface, often seen in semiconductors.[13,22,23,25] On the surface of Ge NWs, a native oxide layer contributes acceptor-like trap states below the intrinsic Fermi level.[21] At equilibrium, these states are filled by electrons, thus promoting hole accumulation near the NW surface, and forming an energetic barrier for electrons to diffuse toward the surface.[24,25,28] At low photoexcited carrier density, the residual electrons trapped in slow states in the surface oxide will attract holes and thus, promote hole trapping in fast surface states at the Ge/oxide interface. On the other hand, electrons must surmount a potential barrier to be trapped in the fast surface states, which tends to enhance the free electron lifetime compared to situation without slow surface states. Figure 3c is a comparison of electron and hole dynamics under low pump power, where both peaks are normalized to maximum, showing that the lifetime of electrons is longer than the lifetime of holes at similar, low pump powers. Comparison with Figure 3a suggests that the lifetime of holes after 10 μJ excitation is even shorter than that for 22 μJ. At high carrier density, more electrons are excited from the slow surface states, which reduces the band bending and hole accumulation effect near the surface,

DOI: 10.1021/acsphotonics.5b00147
ACS Photonics 2015, 2, 1091−1098

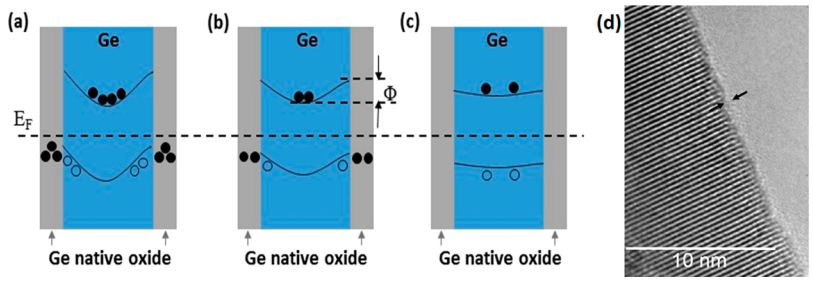

Figure 4. Schematics of electrons trapped in slow surface states of a vertical Ge NW from a cross-sectional view, and a TEM image of an as-grown nanowire surface, showing native oxide. Blue center areas are Ge NW, and gray areas are native oxide layer on Ge NW surface. Note there are fast surface states at the interface of the Ge/native oxide (not shown in these schematics). Slow surface states are produced by defects in the native oxide layer, and are filled by electrons at equilibrium (a). (b, c) Scenarios under low and high power excitation, respectively. Since only some electrons detrap in (b), the barrier Φ for electrons to trap in fast states is higher than the barrier Φ in (c), where the surface slow states are emptied due to high power excitation. (d) The <1 nm native oxide coating of a typical, air-exposed Ge NW.

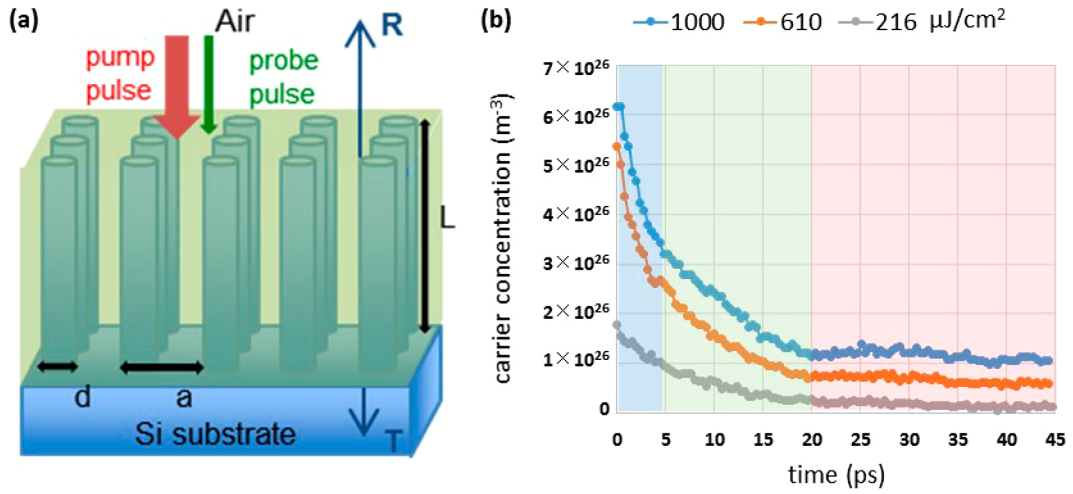

Figure 5. (a) Schematic of an idealized Ge NW array used to simulate the optical response, where the Ge NW array forms an effective medium slab. (b) Carrier concentration dynamics in 40 nm diameter Ge NWs under different pump fluences, which are translated from transient absorption data of Ge NW assemblies using effective medium simulation. Probe wavelength is 470 nm. Background shade colors serve as a guide to view different decay time regimes.

and allows both types of carriers to migrate to the surface. A schematic depiction of electrons trapped in slow surface oxide states under different conditions is shown in Figure 4. A high resolution TEM image of the thin native oxide coating of an air-exposed ⟨111⟩-oriented Ge NW (40 nm nominal diameter) is also shown in Figure 4d. Previously reported synchrotron photoelectron spectroscopy data[29] indicate that this Ge nanowire surface oxide layer is oxygen-deficient relative to GeO_2, consistent with a substantial trap state density that is found to suppress radiative recombination via the indirect gap transition.[30]

Understanding this mechanism is helpful for engineering the photogenerated electron and hole lifetimes in the nanowires. The electron lifetime tends to increase for small NW diameters and low pump powers because electrons that remain trapped in slow surface states produce a barrier for electrons to be trapped in the fast surface states, as evidenced by Figures 3b,c. In contrast, these results suggest that the hole lifetime can be increased by (1) surface passivation to avoid surface native oxide formation on the wires or to produce a less defective surface oxide and oxide/Ge interface, (2) increasing the NW diameter, and (3) exciting the NW using higher power pump pulses. Previous research has indicated that intentional oxidation of native oxide coated Ge NWs produces a more stoichiometric, GeO_2-like, oxide shell that suppresses non-radiative carrier recombination due to surface defects.[31] Moreover, adding a shell of another semiconductor, such as silicon, that exhibits a valence band offset for effective hole confinement away from the wire surface, can shield the Ge core from oxide/semiconductor and bulk oxide defects on the wire surface.[32]

It is worth noting that, after optical excitation empties the slow surface states, electrons trap at these states to achieve equilibrium in a time frame from microseconds to hundreds of seconds.[22,23] By adjusting the pump power levels, even with an ultrashort incident pulse, the increase in the effective electron and hole lifetime can be long-lasting. This has important implications for the electronic and optoelectronic nanowire devices. Although this mechanism was suggested by other reports,[14,23] to the best of our knowledge, Figure 3 is the first experimental evidence of an inverted trend between electron and hole lifetime with increasing carrier concentration in Ge NWs.

In addition to a qualitative interpretation of carrier dynamics from transient absorption data obtained from Ge NW assemblies, we also apply an effective medium simulation model to quantitatively translate the transient absorption of a Ge NW-air metamaterial to time-dependent carrier concen-

DOI: 10.1021/acsphotonics.5b00147
ACS Photonics 2015, 2, 1091−1098

trations. We have demonstrated how to use this tool to simulate transient absorption spectra of Ge NW assemblies, achieving good agreement with experimental observations.[20] To extract carrier concentrations from the transient absorption data, the effective medium theory and the Drude model are combined with the Transfer Matrix Method (TMM) to calculate the induced absorption for the vertically aligned Ge NW arrays. Invoking an effective media model,[20,33] we use an idealized NW assembly, as shown in Figure 5a, to calculate the effective refractive index of actual Ge NW array samples. Nanowires with diameter d are arranged in a square lattice of period a in both x and y directions and have a length L in the z direction. In this report, based on an estimation from SEM images of 40 nm samples, we focus on a structure with such parameters: d = 40 nm, a = 135 nm, and L = 7 μm. Following photoexcitation by the pump pulse, the refractive index of Ge changes with the free carrier concentration, which is accounted for in the effective medium model. Changes in the real part of the index (Δn) and in the imaginary part of index (Δk) produced by a nonequilibrium concentration of electrons (ΔN) and a nonequilibrium concentration of holes (ΔP) can be estimated using the Drude model.[20,34] More details about this simulation approach can be found in ref 20. Figure 5b shows that the extracted time-dependent carrier concentrations decay at different rates under different pump fluences. It is clear that for all pump fluences there are three time regimes: 0−5 ps, 5−20 ps, >20 ps, where the decay rates are different, indicating different dominant recombination mechanisms as discussed below.

Immediately after the pump pulse, due to the high, transient carrier concentration, the photoexcited carriers are expected to recombine rapidly through Auger recombination, where one electron−hole pair gives up its energy to another carrier.[35−38] The rate of this three-body process is therefore cubic in carrier concentration N,

$$\frac{dN}{dt} = -C_3N^3 \quad (1)$$

In order to estimate the Auger coefficient C_3 from a simple linear fitting of extracted carrier concentrations, eq 1 can be rearranged to give

$$[N(t)]^{-2} = 2C_3t + [N(0)]^{-2} \quad (2)$$

We can see that the left-hand side of eq 2 has a linear dependence on the time (t). By plotting $[N(t)]^{-2}$ versus time for the carrier concentrations shown in Figure 5b, we find that data in the time regime of 0−5 ps agree well with a linear fitting, which is expected from the required high carrier concentrations typical of the Auger process.[34,37,38] Figure 6a displays a representative plot of eq 2 for 40 nm samples and a pump fluence of 1 mJ/cm^2. Linear fitting is presented for the probe wavelength 470 nm (2.6 eV). The fitted intercept value gives an estimation of the initial free carrier concentration of 7 × 10^{20} cm^{-3}, consistent with the extracted value in the simulation (6.17 × 10^{20} cm^{-3}). The slope value 2 × 10^{-42} cm^6 ps^{-1} corresponds to $2C_3$ in eq 2, giving an estimated Auger coefficient of about 1 × 10^{-30} cm^6 s^{-1}. Similar values of the Auger coefficient have been reported in multiple references for Ge and Si.[37,38] This agreement is further evidence that, in these photoexcited Ge NW assemblies, Auger recombination dominates the initial fast decay of carrier concentrations for 0−5 ps after excitation. Beyond this time window, carrier concentrations diminish and, therefore, Auger recombination is less prominent than the trapping and recombination of carriers via fast surface states,[13,14,22] as we have shown in Figures 2 and 3.

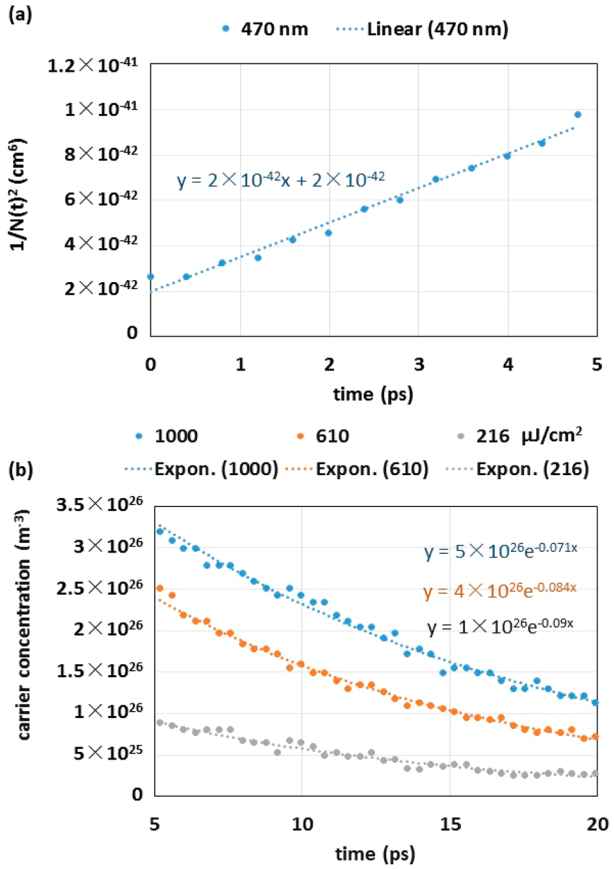

Figure 6. (a) Plots and linear fitting for Auger recombination process in 40 nm samples under a pump fluence of 1 mJ/cm^2 for probe wavelength 470 nm (2.6 eV). An Auger coefficient of about 1 × 10^{-30} cm^6 s^{-1} is estimated. (b) Plots and exponential fitting of carrier concentration in 40 nm diameter Ge NWs under different pump fluences in the time window 5−20 ps, where the fast surface trapping process dominates the decay. Probe wavelength is 470 nm (2.6 eV).

The second time regime shown in Figure 5b, 5−20 ps, can be attributed to recombination via fast surface states at different excitation powers, under the influence of the electrons trapped in the slow surface states of the peripheral oxide, as shown in Figure 4. Here, quantitative analysis is performed by fitting the data to exponential functions to extract lifetimes for carriers under different pump fluences for this time regime. The plotting and fitting shown in Figure 6b indicate an extended carrier lifetime at high pump power, consistent with the behavior of excited holes as discussed above. This hole-behavior of the extracted carrier concentration can be understood by the assumption of the Drude model we used in the simulation.[20] We assumed that the initial nonequilibrium concentration of electrons (ΔN) and nonequilibrium concentration of holes (ΔP) after excitation are equal because the NWs are undoped. However, an energy barrier for electron trapping at fast surface states resulting from electron trapping at slow states in the superficial GeO_x layer will cause electrons and holes to decay at different rates during the relaxation. In fact, the carrier concentrations we extracted (Figures 5 and 6) are weighted averages of electron and hole concentrations, and the weights stand for the relative contributions of electrons and holes to

DOI: 10.1021/acsphotonics.5b00147
ACS Photonics 2015, 2, 1091−1098

induced absorption in the NW-air metamaterial, as shown in the equation

$$\Delta k = \frac{e^3\lambda^3}{16\pi^3 c^3 \varepsilon_0 n}\left(\frac{\Delta N}{\mu_e (m^*_{ce})^2} + \frac{\Delta P}{\mu_h (m^*_{ch})^2}\right) \quad (3)$$

where Δk is the change of the imaginary part of the complex index of refraction of the NW-air metamaterial under study, and k indicates the amount of absorption loss, e is the electron charge, λ is the optical wavelength, c is the speed of light, $\varepsilon_0 = 8.85 \times 10^{-12}$ F·m^{-1}, n is the initial refractive index at λ, m^*_{ce} and m^*_{ch} are the conductivity effective masses, and μ_e and μ_h are the electron and hole mobilities at carrier concentrations ΔN and ΔP. The weights of the electron and hole concentration, are respectively, $(1/(\mu_e(m^*_{ce})^2))$ and $(1/(\mu_h(m^*_{ch})^2))$. The weight of the hole concentration in determining the induced absorption is about 6 times larger than that of electron concentration, based on published values for germanium.[39] Therefore, the extracted carrier concentration decay is expected to have a hole-like dependence on excitation power.

The estimated lifetimes of carriers under different pump fluences for the 5−20 ps regime are shown in Table 1. These

Table 1. Estimated Carrier Lifetimes of 40 nm Diameter Ge NW Assemblies under Different Pump Fluences in the Time Window of 5−20 ps

pump fluence (μJ/cm^2)	lifetime (ps)
1000	14.1
610	11.9
216	11.1

extracted lifetimes clearly decrease as pump fluence decreases, which is consistent with a greater tendency of holes to drift toward the nanowire sidewall surface to recombine at fast surface states, under the influence of trapped negative charge in the surrounding GeO_x surface oxide. Different values of surface recombination lifetime have been reported, from 1 ps to 1 ns, in Ge NWs.[14,15,30] In addition to the NW diameter, the surface composition and chemical bonding also play a critical role in determining the surface recombination lifetime, which explains the variation of reported lifetime values. For the time window beyond 20 ps, as shown in Figure 5b, carrier concentrations decay at slower rates. We suspect that this relatively slow process reflects a combination of fast surface state recombination, and trapping of photogenerated electrons at slow surface states to regain equilibrium after excitation. The latter process influences fast surface recombination.[24,25,28] Further experiments for longer time frames are necessary to verify the time constant of this process occurring at times more than 20 ps after excitation.

In conclusion, we have probed surface recombination of photogenerated carriers in a vertically aligned single crystal Ge NW array-air metamaterial system and have demonstrated diameter-dependent recombination rates and excitation-dependent fast surface recombination rates of pump-induced free carriers. Different responses of electrons and holes to the pump fluence are consistent with the influence of the electrons trapped in slow surface states arising from defects in the native oxide layer on the Ge NWs. Quantitative analysis of Auger recombination and fast surface recombination is possible using an effective medium analysis to connect the transient absorption spectra of the Ge NW array-air metamaterial to time-dependent photogenerated carrier concentrations. Using this simulation tool, we find that (1) the time regime 0−5 ps after excitation is dominated by Auger recombination with an Auger coefficient about 1×10^{-30} cm^6 s^{-1}, (2) the time regime 5−20 ps is dominated by fast surface state recombination with a surface lifetime of ∼13 ps, and (3) the time regime >20 ps is dominated by recombination via both fast and slow surface traps, due to the influence of emptying and trapping of slow surface states. Based on the different responses of electrons and holes to surface recombination versus excitation power, the hole lifetime is longer at higher excitation laser power, while the opposite is true for the electron lifetime. The electron lifetime can be increased by decreasing the NW diameter and reducing the pump power. This is not an intuitive result because, in general, NWs with smaller diameters are more affected by the surface states.[23,26] Here the existence of slow defect states in the surface oxide produces a potential barrier for electrons to be trapped at fast surface states at low pump power. The observed results suggest that the hole lifetime can be increased by (1) avoiding surface native oxide, minimizing the concentration of traps in this oxide or displacing it from the Ge core by adding a shell of another semiconductor to achieves hole confinement, (2) increasing the NW diameter, and (3) exciting the NW by a high power pump pulse. Considering that the trapping time constants reported for slow surface states are in the range of microseconds to hundreds of seconds,[22,23] the enhancement of hole lifetime under high excitation levels is expected to be long-lasting, which may significantly influence the transient optoelectronic characteristics of nanowire devices.

METHODS

Undoped Si(111) substrates (N-type, resistivity >1000 ohm·cm) were used for the NW growth experiments. Commercially available 20, 40, and 80 nm diameter Au colloids (obtained from Ted Pella, Inc.) were diluted by 2% HF with 10:1 colloid to HF volume ratio. Single crystal Si(111) substrates, their surfaces decorated with colloidal Au nanoparticles, were transferred to the load-lock of a cold-walled CVD chamber for NW growth. The lamp-heated, cold-walled CVD system used for the NW growth experiments has been described in a previous publication by Jagannathan et al.[40] A two-temperature growth procedure, which was previously developed for the epitaxial growth of untapered Ge NWs using gold as a catalyst,[41] was employed. The samples were heated up to 365 °C and held at that temperature for 90 s in the presence of GeH_4 diluted with H_2. The subsequent growth step temperature was at 300 °C, with a duration of 60 min, producing wires of ∼7 μm length. The total pressure inside the reactor chamber was 30 Torr, with GeH_4 partial pressure of 0.75 Torr. The diameters of Ge NWs are mainly determined by, and slightly larger than, the diameters of the Au catalysts due to Au particles coarsening prior to wire nucleation.[42] More details about sample preparation are described in another paper.[20]

In the ultrafast TA experiment described here, the pump wavelength was 780 nm (1.59 eV) with a pulse duration around 230 fs, as determined by autocorrelation. Similar pulse durations have been found for the different probe wavelengths we used in this study. All experiments were performed at room temperature with vertically polarized pump and probe pulses, near normal incidence to the substrate. The probe is detected after reflection from the sample substrate by a homemade integrating photodiode, coupled with a fast data acquisition

DOI: 10.1021/acsphotonics.5b00147
ACS Photonics 2015, 2, 1091−1098

card. A mechanical chopper, inserted in the pump line, is operated at half the laser repetition rate (500 Hz) and allows a pump-on/pump-off configuration to determine the change in reflection coefficient induced by the pump pulse. As the reflection of the probe pulse occurs mainly at the Si substrate, the NWs are effectively measured in transmission. More details about the ultrafast TA experiment setup can be found elsewhere.[20]

AUTHOR INFORMATION

Corresponding Author

*E-mail: pcm1@stanford.edu.

Notes

The authors declare no competing financial interest.

ACKNOWLEDGMENTS

We acknowledge the financial support of the National Science Foundation (DMR 1206511).

REFERENCES

(1) Camacho-Aguilera, R. E.; Cai, Y.; Patel, N.; Bessette, J. T.; Romagnoli, M.; Kimerling, L. C.; Michel, J. An Electrically Pumped Germanium Laser. *Opt. Express* **2012**, *20*, 11316.

(2) Liu, J.; Sun, X.; Camacho-Aguilera, R.; Kimerling, L. C.; Michel, J. Ge-on-Si Laser Operating at Room Temperature. *Opt. Lett.* **2010**, *35*, 679−681.

(3) Boztug, C.; Sánchez-Pérez, J. R.; Cavallo, F.; Lagally, M. G.; Paiella, R. Strained-Germanium Nanostructures for Infrared Photonics. *ACS Nano* **2014**, *8*, 3136−3151.

(4) Oehme, M.; Gollhofer, M.; Widmann, D.; Schmid, M.; Kaschel, M.; Kasper, E.; Schulze, J. Direct Bandgap Narrowing in Ge LED's on Si Substrates. *Opt. Express* **2013**, *21*, 2206−2211.

(5) Lockwood, D. J.; Tsybeskov, L. Fast Light-Emitting Silicon-Germanium Nanostructures for Optical Interconnects. *Opt. Quantum Electron.* **2012**, *44*, 505−512.

(6) Polyakov, B.; Daly, B.; Prikulis, J.; Lisauskas, V.; Vengalis, B.; Morris, M. A.; Holmes, J. D.; Erts, D. High-Density Arrays of Germanium Nanowire Photoresistors. *Adv. Mater.* **2006**, *18*, 1812−1816.

(7) Li, G.; Luo, Y.; Zheng, X.; Masini, G.; Mekis, A.; Sahni, S.; Thacker, H.; Yao, J.; Shubin, I.; Raj, K.; et al. Improving CMOS-Compatible Germanium Photodetectors. *Opt. Express* **2012**, *20*, 26345−26350.

(8) Assefa, S.; Xia, F.; Vlasov, Y. A. Reinventing Germanium Avalanche Photodetector for Nanophotonic on-Chip Optical Interconnects. *Nature* **2010**, *464*, 80−84.

(9) Ren, F. F.; Ang, K. W.; Ye, J.; Yu, M.; Lo, G. Q.; Kwong, D. L. Split Bull's Eye Shaped Aluminum Antenna for Plasmon-Enhanced Nanometer Scale Germanium Photodetector. *Nano Lett.* **2011**, *11*, 1289−1293.

(10) Tang, L.; Kocabas, S. E.; Latif, S.; Okyay, A. K.; Ly-Gagnon, D.-S.; Saraswat, K. C.; Miller, D. A. B. Nanometre-Scale Germanium Photodetector Enhanced by a near-Infrared Dipole Antenna. *Nat. Photonics* **2008**, *2*, 226−229.

(11) Lo, S. S.; Major, T. a; Petchsang, N.; Huang, L.; Kuno, M. K.; Hartland, G. V. Charge Carrier Trapping and Acoustic Phonon Modes in Single CdTe Nanowires. *ACS Nano* **2012**, *6*, 5274−5282.

(12) Prasankumar, R. P.; Upadhya, P. C.; Taylor, A. J. Ultrafast Carrier Dynamics in Semiconductor Nanowires. *Phys. Status Solidi B* **2009**, *246*, 1973−1995.

(13) Calarco, R.; Marso, M.; Richter, T.; Aykanat, A. I.; Meijers, R.; Hart, A. v. d.; Stoica, T.; Lüth, H. Size-Dependent Photoconductivity in MBE-Grown GaN−Nanowires. *Nano Lett.* **2005**, *5*, 981−984.

(14) Prasankumar, R. P.; Choi, S.; Trugman, S. a; Picraux, S. T.; Taylor, a J. Ultrafast Electron and Hole Dynamics in Germanium Nanowires. *Nano Lett.* **2008**, *8*, 1619−1624.

(15) Strait, J. H.; George, P. A.; Levendorf, M.; Blood-Forsythe, M.; Rana, F.; Park, J. Measurements of the Carrier Dynamics and Terahertz Response of Oriented Germanium Nanowires Using Optical-Pump Terahertz-Probe Spectroscopy. *Nano Lett.* **2009**, *9*, 2967−2972.

(16) Allen, J. E.; Hemesath, E. R.; Perea, D. E.; Lensch-Falk, J. L.; Li, Z. Y.; Yin, F.; Gass, M. H.; Wang, P.; Bleloch, A. L.; Palmer, R. E.; et al. High-Resolution Detection of Au Catalyst Atoms in Si Nanowires. *Nat. Nanotechnol.* **2008**, *3*, 168−173.

(17) Harris, C.; O'Reilly, E. P. Nature of the Band Gap of Silicon and Germanium Nanowires. *Phys. E* **2006**, *32*, 341−345.

(18) Haight, R.; Sirinakis, G.; Reuter, M. Photoelectron Spectroscopy of Individual Nanowires of Si and Ge. *Appl. Phys. Lett.* **2007**, *91*, 233116.

(19) Cohen, M.; Bergstresser, T. Band Structures and Pseudopotential Form Factors for Fourteen Semiconductors of the Diamond and Zinc-Blende Structures. *Phys. Rev.* **1966**, *141*, 789−796.

(20) Li, Y.; Clady, R.; Park, J.; Thombare, S. V.; Schmidt, T. W.; Brongersma, M. L.; McIntyre, P. C. Ultrafast Electron and Phonon Response of Oriented and Diameter-Controlled Germanium Nanowire Arrays. *Nano Lett.* **2014**, *14*, 3427−3431.

(21) Zhang, S.; Hemesath, E. R.; Perea, D. E.; Wijaya, E.; Lensch-Falk, J. L.; Lauhon, L. J. Relative Influence of Surface States and Bulk Impurities on the Electrical Properties of Ge Nanowires. *Nano Lett.* **2009**, *9*, 3268−3274.

(22) Kingston, R. H. Review of Germanium Surface Phenomena. *J. Appl. Phys.* **1956**, *27*, 101−114.

(23) Hanrath, T.; Korgel, B. A. Influence of Surface States on Electron Transport through Intrinsic Ge Nanowires. *J. Phys. Chem. B* **2005**, *109*, 5518−5524.

(24) Rupprecht, G. Measurement of Germanium Surface States by Pulsed Channel Effect. *Phys. Rev.* **1958**, *111*, 75−81.

(25) Bardeen, J. Surface States and Rectification at a Metal Semi-Conductor Contact. *Phys. Rev.* **1947**, *71*, 717−727.

(26) Léonard, F.; Talin, A.; Swartzentruber, B.; Picraux, S. T. Diameter-Dependent Electronic Transport Properties of Au-Catalyst/Ge-Nanowire Schottky Diodes. *Phys. Rev. Lett.* **2009**, *102*, 106805.

(27) Lo, S. S.; Devadas, M. S.; Major, T. A.; Hartland, G. V. Optical Detection of Single Nano-Objects by Transient Absorption Microscopy. *Analyst* **2013**, *138*, 25−31.

(28) Ahn, H.; Yu, C.-C.; Yu, P.; Tang, J.; Hong, Y.-L.; Gwo, S. Carrier Dynamics in InN Nanorod Arrays. *Opt. Express* **2012**, *20*, 769.

(29) Adhikari, H.; McIntyre, P. C.; Sun, S. Y.; Pianetta, P.; Chidsey, C. E. D. Photoemission Studies of Passivation of Germanium Nanowires. *Appl. Phys. Lett.* **2005**, *87*, 263109.

(30) Kawamura, Y.; Huang, K. C. Y.; Thombare, S. V.; Hu, S.; Gunji, M.; Ishikawa, T.; Brongersma, M.; Itoh, K. M.; McIntyre, P. C. Direct-Gap Photoluminescence from Germanium Nanowires. *Phys. Rev. B* **2012**, *86*, 035306.

(31) Hashemi, F. S. M.; Thombare, S.; Fontcuberta i Morral, A.; Brongersma, M. L.; McIntyre, P. C. Effects of Surface Oxide Formation on Germanium Nanowire Band-Edge Photoluminescence. *Appl. Phys. Lett.* **2013**, *102*, 251122.

(32) Hu, S.; Kawamura, Y.; Huang, K. C. Y.; Li, Y.; Marshall, A. F.; Itoh, K. M.; Brongersma, M.; McIntyre, P. C. Thermal Stability and Surface Passivation of Ge Nanowires Coated by Epitaxial SiGe Shells. *Nano Lett.* **2012**, *12*, 1385.

(33) Xiong, Z.; Zhao, F.; Yang, J.; Hu, X. Comparison of Optical Absorption in Si Nanowire and Nanoporous Si Structures for Photovoltaic Applications. *Appl. Phys. Lett.* **2010**, *96*, 181903.

(34) Soref, R. A.; Friedman, L. Electro-Optical Modulation in SiGeSi and Related Heterostructures. *Int. J. Optoelectron.* **1994**, *9*, 205−210.

(35) Robel, I.; Bunker, B. A.; Kamat, P. V.; Kuno, M. Exciton Recombination Dynamics in CdSe Nanowires: Bimolecular to Three-Carrier Auger Kinetics. *Nano Lett.* **2006**, *6*, 1344−1349.

(36) Vietmeyer, F.; McDonald, M. P.; Kuno, M. Single Nanowire Microscopy and Spectroscopy. *J. Phys. Chem. C* **2012**, *116*, 12379−12396.

DOI: 10.1021/acsphotonics.5b00147
ACS Photonics 2015, 2, 1091−1098

(37) Nilsson, N. G. Band-to-Band Auger Recombination in Silicon and Germanium. *Phys. Scr.* **1973**, *8*, 165−176.
(38) Conradt, R.; Aengenheister, J. Minority Carrier Lifetime in Highly Doped Ge. *Solid State Commun.* **1972**, *10*, 321−323.
(39) Madelung, O. *Semiconductors: Group IW Elements and III-V Compounds*; Springer-Verlag: Berlin, 1991; pp 5−57.
(40) Jagannathan, H.; Deal, M.; Nishi, Y.; Woodruff, J.; Chidsey, C. E. D.; McIntyre, P. C. Nature of Germanium Nanowire Heteroepitaxy on Silicon Substrates. *J. Appl. Phys.* **2006**, *100*, 024318.
(41) Adhikari, H.; Marshall, A. F.; Chidsey, C. E. D.; McIntyre, P. C. Germanium Nanowire Epitaxy: Shape and Orientation Control. *Nano Lett.* **2006**, *6*, 318−323.
(42) Koto, M.; Marshall, A. F.; Goldthorpe, I. a; McIntyre, P. C. Gold-Catalyzed Vapor-Liquid-Solid Germanium-Nanowire Nucleation on Porous Silicon. *Small* **2010**, *6*, 1032−1037.

DOI: 10.1021/acsphotonics.5b00147
ACS Photonics 2015, 2, 1091−1098